

## Original Article

# The prognostic value and multiomic features of m6A-related risk signature in lung adenocarcinoma

Xiangcheng Wang<sup>1\*</sup>, Qin Yu<sup>2,3\*</sup>, Hongfang Yu<sup>2,3</sup>, Yuzhe Wang<sup>2,3</sup>, Liping Sun<sup>2,3</sup>, Lei Yu<sup>4</sup>, Hongwei Cui<sup>5,6</sup>, Hao Yang<sup>2,3</sup>

<sup>1</sup>Department of Nuclear Medicine, Shenzhen People's Hospital, Shenzhen 518020, Guangdong, China;

<sup>2</sup>Department of Radiation Oncology, Inner Mongolia Cancer Hospital & Affiliated People's Hospital of Inner Mongolia Medical University, Huhhot 010020, Inner Mongolia Autonomous Region, China; <sup>3</sup>The Laboratory of Radiation Physics and Biology, Affiliated People's Hospital of Inner Mongolia Medical University & Inner Mongolia Cancer Hospital, Huhhot 010020, Inner Mongolia Autonomous Region, China; <sup>4</sup>Department of Pharmacy, Traditional Chinese Medicine Hospital of Inner Mongolia Autonomous Region, Hohhot 010020, Inner Mongolia Autonomous Region, China; <sup>5</sup>Scientific Research Department, Inner Mongolia Cancer Hospital & Affiliated People's Hospital of Inner Mongolia Medical University, Huhhot 010020, Inner Mongolia Autonomous Region, China; <sup>6</sup>Clinical Research Center, The Affiliated Hospital of Inner Mongolia Medical University, Huhhot 010050, Inner Mongolia Autonomous Region, China. \*Equal contributors and co-first authors.

Received April 13, 2022; Accepted June 29, 2022; Epub August 15, 2022; Published August 30, 2022

**Abstract:** Objectives: N<sup>6</sup>-methyladenosine (m6A), a predominant RNA modification, has been recently linked to messenger RNA splicing, stability and expression, and its dysregulation may be important in the initiation as well as development of human cancers. The current study was proposed to investigate the clinico-pathological value and multiomic characteristics of m6A-linked genes in the diagnosis and prognosis of lung adenocarcinoma (LUAD). Methods: The expression levels and mutation types of 21 previously identified m6A regulators were analyzed using the TCGA (The Cancer Genome Atlas) database. The patients were categorized into two groups, a training group (n=392) and a testing group (n=98). Next, the prognostic score of m6A regulators was determined by the Cox survival analysis and a regression model of LASSO to develop a risk profile for patients with LUAD. Moreover, features of risk signature, including chemosensitivity, tumor immune microenvironment and genetic mutation, were also explored. Results: In total, 18 of 21 m6A regulators showed significantly differential expression in LUAD (P<0.05). Among them, 6 genes were observed to be associated with the Overall Survival (OS) of patients with LUAD. Three genes (IGF2BP1 and 2, and HNRNPC) were further evaluated as a prognostic signature in LUAD. Patients, grouped as high risk based on the median of risk score, had poorer OS in comparison with those in low-risk group (P<0.05). The accuracy of our prognostic signatures was high: the AUC were 0.67, 0.59, 0.64 (training set), and 0.65, 0.69, 0.64 (testing set) at survival of 1-, 3- and 5-year, respectively. The prognostic performance of IGF2BP1, IGF2BP2 and HNRNPC was successfully validated in two independent external cohorts. High-risk score was an indicator of chemoresistance, TP53 mutation and increased infiltration of immune cells, and *in vitro* assessment of the cellular function of HNRNPC confirmed that the gene is involved in cell proliferation and invasion. Conclusion: The prognostic signature based on m6A regulators might provide novel insights into prognostic assessment and individualized treatment for patients with LUAD.

**Keywords:** Lung adenocarcinoma (LUAD), N6-methyladenosine (m6A), prognostic signature, HNRNPC, TCGA

## Introduction

The recently presented global cancer statistics have pinpointed lung cancer to be the most commonly occurring cancer around the globe [1, 2]. In China, the recent statistical analysis has demonstrated an upward trend in the total number of patients suffering with lung cancer,

which is undoubtedly an alarming situation that needs to be tackled properly to avoid severe public health emergency [3]. It cannot be ignored that the technological development and increasing awareness of intermittent screening of lung cancer has helped medical fraternity to develop personalized treatment strategies, but early identification and timely

prognosis are still the two major challenges that exist today. Studies have further demonstrated that a survival rate of 5 years is observed only in 10% patients with stage IV lung cancer. Thus, it is quite a need of an hour to explore novel genomic predictive tools for early identification, along with novel follow-up or post-surgery strategies for better therapeutic outcome.

Genomic analysis is a novel tool for identifying various signaling pathways that may lead to cancerous development once triggered by external sources. Studies have indicated that various ribonucleic acid modifications present in more complex eukaryotes, among which N6-methyladenosine (m6A) is commonly studied. The said modifier is identified to be an important player in regulating messenger RNA splicing, which can further impact on RNA stability as well as post-transcriptional modifications [5-7]. The epigenetic changes associated with adenosine methylation at N6 position of the said modifier are identified to be associated with methyltransferases, known as writers and demethylases, recognized as erasers along with binding proteins that are known to be proofreaders [8]. Further studies in the same direction have proposed that the dysregulation in the process of m6A associated RNA modification can have direct impact on various pathological processes, such as development and progression of different cancers [9, 10]. Furthermore, the involvement of m6A modifiers in the therapeutic modalities have been thought to be very useful in many therapeutic interventions.

For that instance, a recent study has proposed that epigenetic modifications facilitated by blocking m6A-modified can inhibit the cellular proliferation by blocking insulin-like growth factor 2 (ILGF), along with the migration and invasion of bladder cancer [11]. Nevertheless, Yu et al. further documented that the expression level of AlkB homolog 5 (ALKBH5), which is noted as an eraser protein, was significantly low in bladder cancer samples, and confirmed that the increased expression of ALKBH5 could suppress progression of bladder cancer and increase chemosensitivity towards cisplatin, in an m6A-dependent manner [12]. Overall, these findings indicate that m6A-binding protein can be exploited as an effective diagnostic as well

as prognostic marker for patients suffering from different cancers to obtain a better therapeutic outcome.

The present study intended to understand the expression profile along with molecular features of genes related to m6A using The Cancer Genome Atlas i.e., TCGA database, and we further defined genetic signatures based on m6A related genes specific for lung cancer.

## Materials and methods

### *Data source expression analysis*

The TCGA database was used for downloading fragments per kilobase of transcripts per million expression data (FPKM), along with clinico-pathological information of 594 specimens obtained from patients with lung adenocarcinoma (LUAD). Out of the 594 biopsy specimens, 535 were tumor biopsy and 59 were control samples (<https://portal.gdc.cancer.gov/>). Based on previous findings, a set of 21 m6A modifiers were selected [8, 13], including 10 binding proteins (IGF2BP1, YTHDF1, IGF2BP2, YTHDF2, IGF2BP3, YTHDF3, HNRNPA2B1, HNRNPC, YTHDC1 and YTHDC2). The selected modifiers also contained 9 methyltransferases (WTAP, RBM15, RBM15B, RBMX, METTL3, METTL14, METTL16, ZC3H13, VIRMA and 2-demethylases (ALKBH5 and FTO)). Tools like differential gene expression analysis were utilized to extract expression values of specific m6A pathway related genes, which were compared with LUAD tissues and adjacent control tissues. The “limma R” package was used to qualify data from differential gene expression. The significant criteria were set to  $|\log \text{ Fold Change (LFC)}| > 1$  and adjusted  $P$ -value ( $\text{padj}$ )  $< 0.05$ . Additionally, two more datasets GSE-50081 ( $n=127$  patients) and GSE30219 ( $n=83$  patients) were referred as independent external validation cohorts [14, 15]. The Gene Expression Omnibus (GEO) database was utilized for downloading follow-up information of corresponding patient data (<https://www.ncbi.nlm.nih.gov/geo/>).

Additionally, Gene Expression Profiling Interactive Analysis was exploited to get the idea about expression level of m6A pathway related genes in 33 types of pan-cancer samples. It should be noted that the Gene Expression Profiling is a virtual tool used to analyze expres-

sion profile of gene from different types of cancers and to compare that with the profile obtained from non-cancerous specimen.

## *Mutation analysis of genes associated with m6A in LUAD samples*

The direct association between numerical variation of somatic copy and mRNA expression of m6A pathway-linked genes was analyzed with the help of cBioPortal for Cancer Genomics (<http://www.cbioportal.org>) [16].

## *Development of a prognostic gene expression signature using a subset of m6A pathway-related genes*

The correlation between overall survival (OS) of patients with LUAD and m6A-linked gene transcription was identified using the Univariate Cox regression. Least absolute shrinkage and selection operator (LASSO) was used as a regression model to identify useful candidates for prognostic construction of gene expression signatures, in consideration of m6A-related genes. The risk score was determined according to the basis of the extent of transcription in selected gene and the corresponding coefficient. The previously selected patients with LUAD were categorized into high- and low-risk sets based on the computer median risk score calculated by formerly mentioned m6A-related prognostic signature.

## *Evaluation of infiltration of immune cells and drug sensitivity*

The evaluation of extent of immune cell infiltration was conducted on the patients in both high and low risk groups. Further analysis on number of patients (n=22) was carried out using CIBERSORT algorithm [17]. The other data depending upon the sensitivity of chemotherapeutic drug was obtained from reference database, Genomics of Drug Sensitivity in Cancer (GDSC) database (<https://www.cancerrxgene.org/downloads>) [18]. The response to chemotherapy drugs for each tumor sample was expressed as 50% of cellular growth inhibition (IC50) and was determined with the “pRRophetic” software of R.

## *Gene ontology (GO) and gene set variation analysis (GSVA)*

The analysis of GO enrichment along with GSVA tools were used to identify underlying signaling

pathways associated with LUAD risk modifications. In order to explain this in brief, the hallmarks of signature pathways were downloaded from reference database i.e., the Molecular Signatures Database (MsigDB). The gene enrichment score was calculated in samples with high and low risk. The functional annotation and GO enrichment analysis were conducted on the gene sets that were expressed at significantly different levels between high and low risk categories. The *p*-value and false discover rate (FDR) score were defined in each case, and *p*<0.05 was considered to be statistically significant.

## *In vitro cell culture analysis and transient transfection*

The human cell lines like LUAD (A549, LLC, HUH7) and lung epithelial cell (BEAS-2B) normal tissue were obtained from the Department of Biochemistry and Cell Biology, the Institute of Chinese Academy of Science. The relevant cell cultivation was accomplished following standard culture protocols. Briefly, all cells were expanded in DMEM (Invitrogen, USA) containing 10% fetal bovine serum (FBS) (GIBCO, USA) and cultured at 37°C in an incubator with humidity and 5% CO<sub>2</sub>. The ectopic downregulation and/or upregulation of expression profile of HNRNPC in LUAD cells were modified with newly designed small interfering RNA (siRNA) and pcDNA3.1 vector with specific heterogeneous nuclear ribonucleoprotein C1/C2. The sequences of siRNA against HNRNPC were as follows: sense: 5'-GCGCUUGUCUAAGAUCAAA-UU-3'; antisense: 5'-AAUUUGAUCUUAGACAAG-CGC-3'; sense for siRNA-negative control (NC): 5'-UUCUCCGAACG UGUCACGU-3'; antisense for siRNA-NC: 5'-ACGUGACA CGUUCGG AGAA-3'. Cell transfection was conducted in a 6-well plate (5 × 10<sup>5</sup> cells/well) using the lipofectamine 3000.

## *Colony formation, wound healing and transwell invasion assay*

The growth of LUAD cells in gain- and loss-of function experiments was assessed using colony formation assay. In brief, approximately 100 cells were plated per well onto 12-well plates and grew for 14 days in standard culture condition. The cells were then counted after fixation using crystal violet (0.1%). The migration ability of cells obtained from LUAD was detected with

the help of wound healing assay, and transfected cells were expanded in 6-well plates with a plating density of  $5 \times 10^5$  cells per well. The cells were incubated at 37°C for 24 h. Furthermore, a linear wound was created artificially by a 200 µl pipette tip. After washing 3 times with PBS, we then incubated cells in a medium with no serum for additional 24 h. The number of migrative cells was quantified by counting under a light microscope (Olympus, Japan).

For the Transwell invasion assay, 100 µL Matrigel (Corning, USA) diluted with culture medium was coated in the upper chambers. On the matrigel coating approximately  $5 \times 10^4$  cells were seeded along with serum-free medium. In contrast, the bottom chambers were treated as controls. The controls were expanded in plain DMEM with 10% FBS. After 48 h incubation, cells in the lower chamber were fixed with 4% paraformaldehyde (PFA) and stained by crystal violet. The images of invasive cells were captured by a light microscope (Olympus, Japan).

#### Statistical analysis

The significance of the changes in the transcription of m6A-related genes between LUAD and adjacent normal samples was assessed using the Wilcoxon rank-sum test. The prognostic value of m6A-pathway related gene signature was calculated using Kaplan-Meier method. The difference in survival between low and high-risk groups was compared using a two-sided log-rank test. Sensitivity and specificity of the m6A-related prognostic signature were further assessed using receiver operating characteristic (ROC) curves and the values of area under the curve (AUC). The univariate and multivariate Cox regression analysis were conducted to determine the prognostic factors of patients with LUAD. Data processing and statistical analysis were performed using R 3.6.1 (<http://www.rproject.org/>). Two-tailed *P*-value of <0.05 was considered statistically significant.

## Results

### *Transcription and genetic modification of m6A-related genes in LUAD samples*

As described previously, 21 m6A modifiers were selected and characterized. A correlation

analysis demonstrated a robust correlation between the expression of VIRMA and YTHDF3 (correlation coefficient =0.75) (**Figure 1A**). Next, we assessed the expression levels of m6A-related genes in LUAD samples referring the expression data from the TCGA cohort and compared the mutation frequency of the selected 21 genes. As shown in **Figure 1B**, 18 of 21 m6A modifiers were differentially expressed in tumor tissues as compared to that of the control ( $P<0.05$ ). Among them, the mutation frequency of YTHDF1 was 28% in 404 LUAD samples, the highest among the studied genes (**Figure 1C**).

### *Consensus clustering of m6A-related genes in LUAD samples*

All patients with LUAD were clustered into groups as per the expression levels of m6A-linked genes. The clustering stability was determined by the consensus matrix *k* value (from *k*=2 to *k*=9), and the results indicated that the highest clustering stability and the least crossover were observed when the *k* value was equal to 2 (**Figure 2A-C**). Therefore, LUAD samples were clustered into 2 primary groups (primarily cluster 1 and 2) on the basis of differential levels of genetic expression of m6A-related genes. The outcomes of principal component analysis (PCA) revealed that the two subgroups could be clearly distinguished by the clustering model of m6A-related genes (**Figure 2D**). The Kaplan-Meier curve confirmed that the OS of cluster 2 was considerably shorter in comparison to that of the cluster 1 ( $P=0.001$ ). See **Figure 2E**.

### *Developing and validating m6A pathway-related diagnostic markers*

To establish the limit of prognostic detection of the m6A-related genes, first, the Cox regression analysis was carried out on the TCGA dataset. The final outcome identified six genes, including IGF2BP1, IGF2BP3, IGF2BP2, HNRNPC, heterogeneous nuclear ribonucleoprotein A2B1 (HNRNPA2B1) and RNA-binding motif protein 15 (RBM15), which were linked with the early diagnosis and therapeutic outcome of patients with LUAD. Then, these m6A-related genes were further assessed to optimize risk characteristics using the LASSO regression model (**Figure 3A, 3B**). Ultimately, IGF2BP1, IGF2BP2 and HNRNPC were selected to develop a prognostic gene signature for patients with



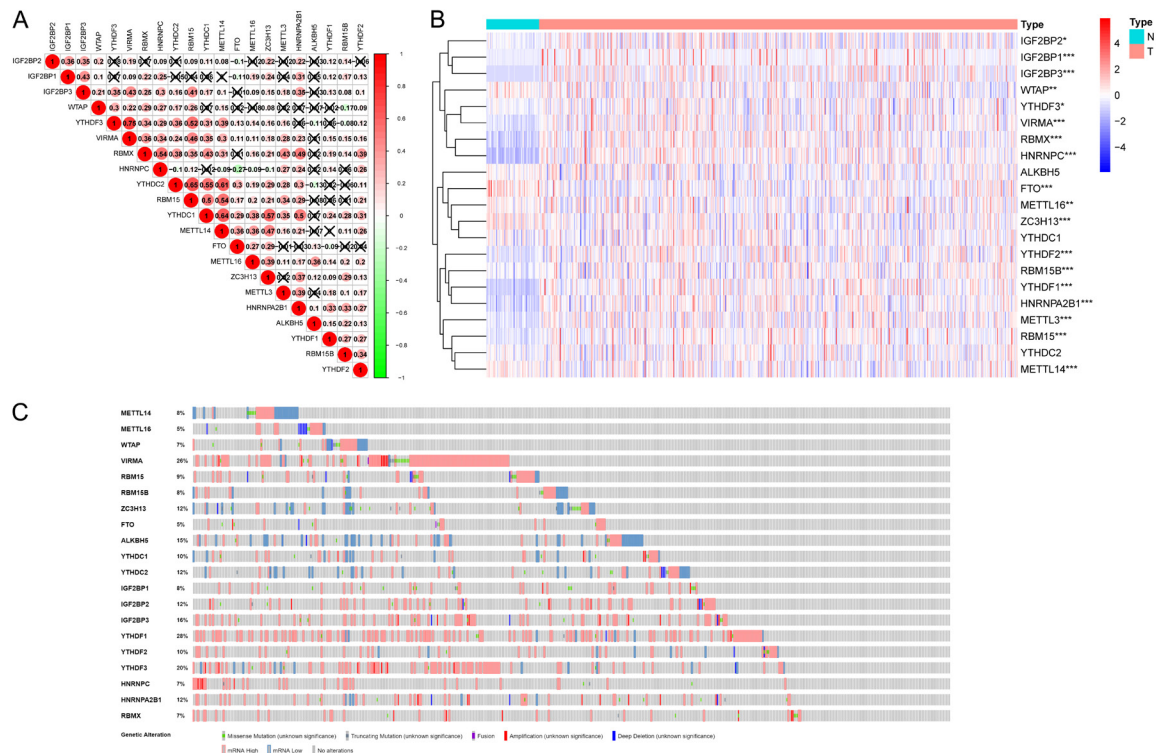


**Figure 1.** A. The expression correlations among 21 m6A-related genes; B. The expression heatmap of 21 m6A-related genes in lung adenocarcinoma (LUAD) samples; C. The mutation patterns of 21 m6A-associated genes in LUAD samples. \* $P < 0.05$ , \*\* $P < 0.01$ , and \*\*\* $P < 0.001$ .

LUAD (Figure 3C). Considering the mRNA expression level of the three selected genes, the risk score characterized with diagnostic signature was analyzed by the formula  $(IGF2BP1 \times 0.0883) + (IGF2BP2 \times 0.0444) + (HNRNP2B1 \times 0.0312)$ .

To detect the prognostic significance of these gene expression markers, we randomly assigned 490 LUAD samples obtained via the TCGA dataset as a training ( $n=392$ ) set or a testing ( $n=98$ ) set. Two patient cohorts were further divided into low- and high-risk groups based on the median of calculated risk score. Kaplan-Meier curve analysis confirmed that the high risk group reported low OS in comparison with the low-risk patients ( $P < 0.001$ ) (Figure 3D). The findings obtained in the testing set were similarly comparable, indicating that the high-risk score can be a predictor of poor OS in patients with LUAD ( $P < 0.05$ ) (Figure 3E). Moreover, the ROC curves showed that the hallmarks of prognosis based on three m6A-related genes had a good predictive accuracy for patients with LUAD. The data further suggested that the AUC value of 1-, 3-, and 5-year OS was 0.67, 0.59 and 0.64, respectively in the training set

(Figure 3D). The AUC value of 1-, 3- and 5-year OS was 0.65, 0.69 and 0.64, respectively in the testing set (Figure 3E). The Cox regression analysis, in both univariate as well as multivariate forms revealed that TNM stage and risk signature of 3 m6A-related genes could be considered as independent prognostic predictors for patients with LUAD in the TCGA dataset (Figure 3F, 3G). A prognostic nomogram for patients with LUAD has been established according to the variables identified by the Cox regression analysis. The results showed that the nomogram had a good predictive performance, with a C-index of 0.727.

Furthermore, two independent external cohorts (GSE50081 and GSE30219) confirmed the diagnostic importance of the m6A-associated signature. In accordance with the risk score of the diagnostic hallmarks, the GSE50081 dataset included 63 high-risk and 64 low-risk patients, and GSE30219 dataset included 41 high-risk and 42 low-risk patients. The survival curves consistently showed that the OS of high-risk patients was shorter than that of the other counterparts in both GSE50081 ( $P < 0.001$ ) and GSE30219 datasets ( $P = 0.005$ )

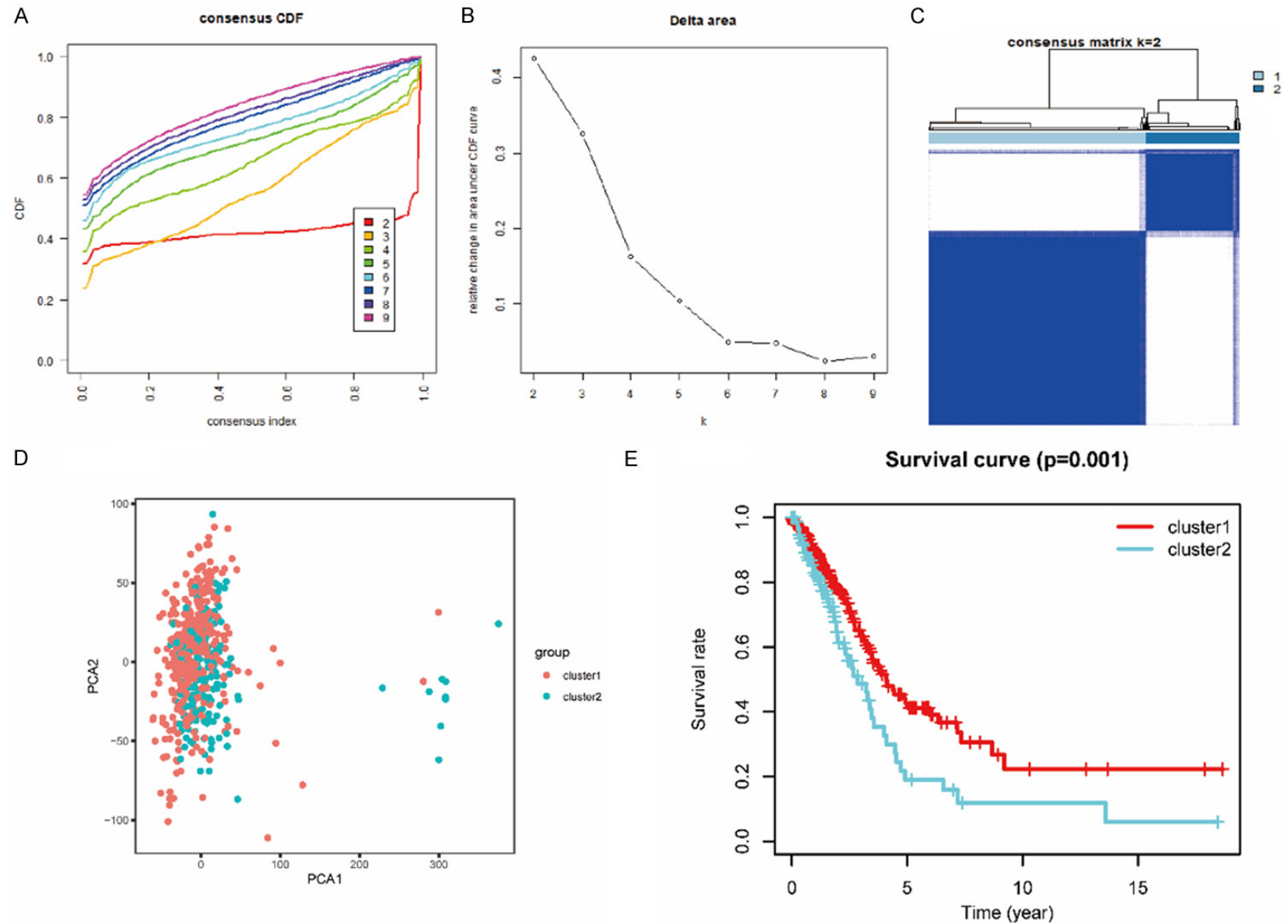


**Figure 2.** A. Cumulative distribution function of consensus clustering (k=2 to 9); B. Relative change in area under CDF curve and tracking plot (k=2 to 9); C. The patients with lung adenocarcinoma (LUAD) from the TCGA dataset were clustered into different groups (k=2). D. Principal component analysis (PCA) of the expression profile of m6A regulators; E. The different survival between clusters 1 and 2 plotted by Kaplan-Meier curve.

# M6A and lung adenocarcinoma

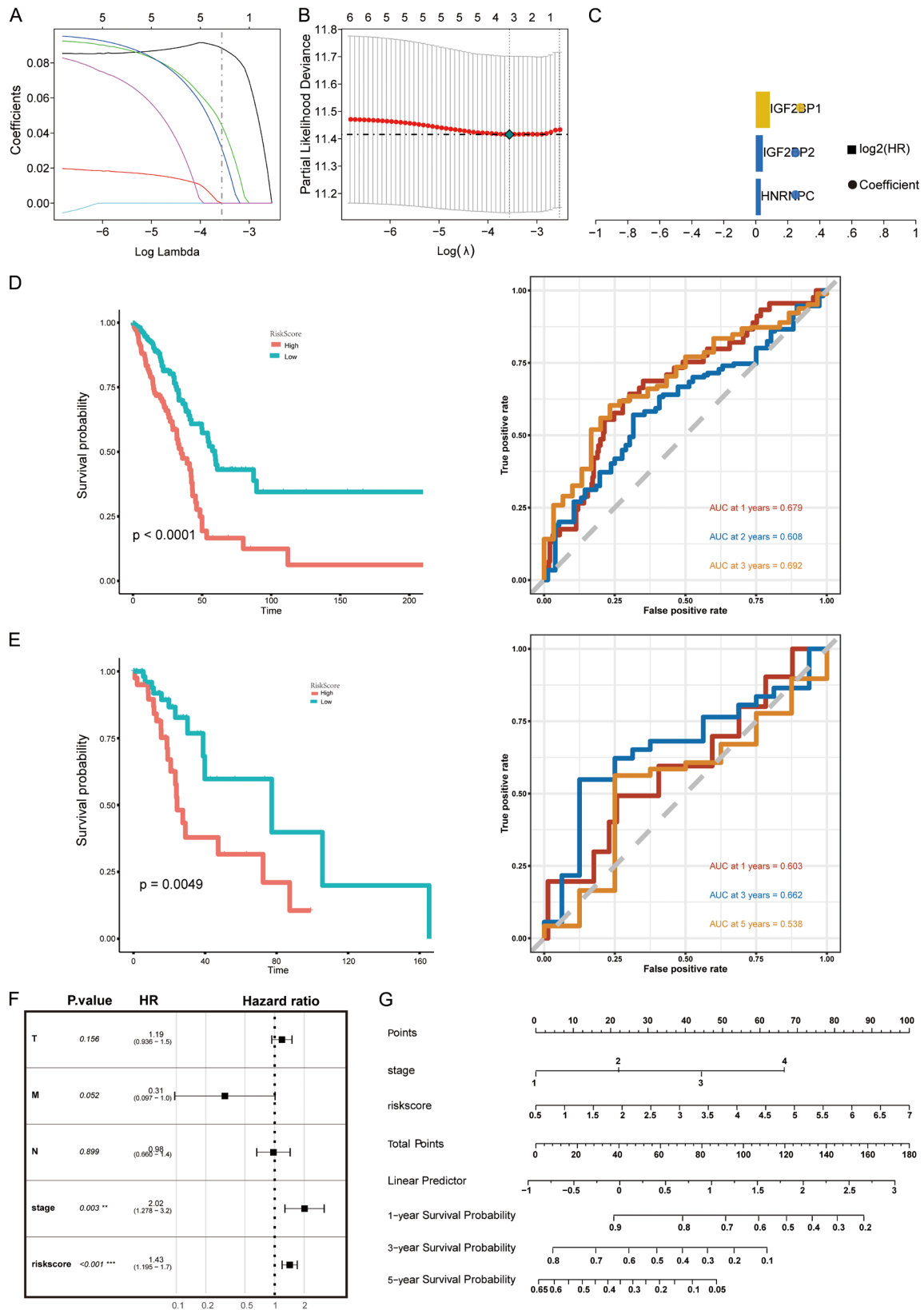


**Figure 3.** (A-C) Lasso regression model was used to develop a prognostic signature of m6A regulators for patients with LUAD; (D, E) The prognostic value of three m6A-related signature for the training set (n=392) and testing set (n=98) was evaluated by the Kaplan-Meier curves and receiver operating characteristic curves, respectively. The prognostic factors for patients with LUAD from the TCGA dataset were determined by univariate (F) and multivariate Cox regression (G).

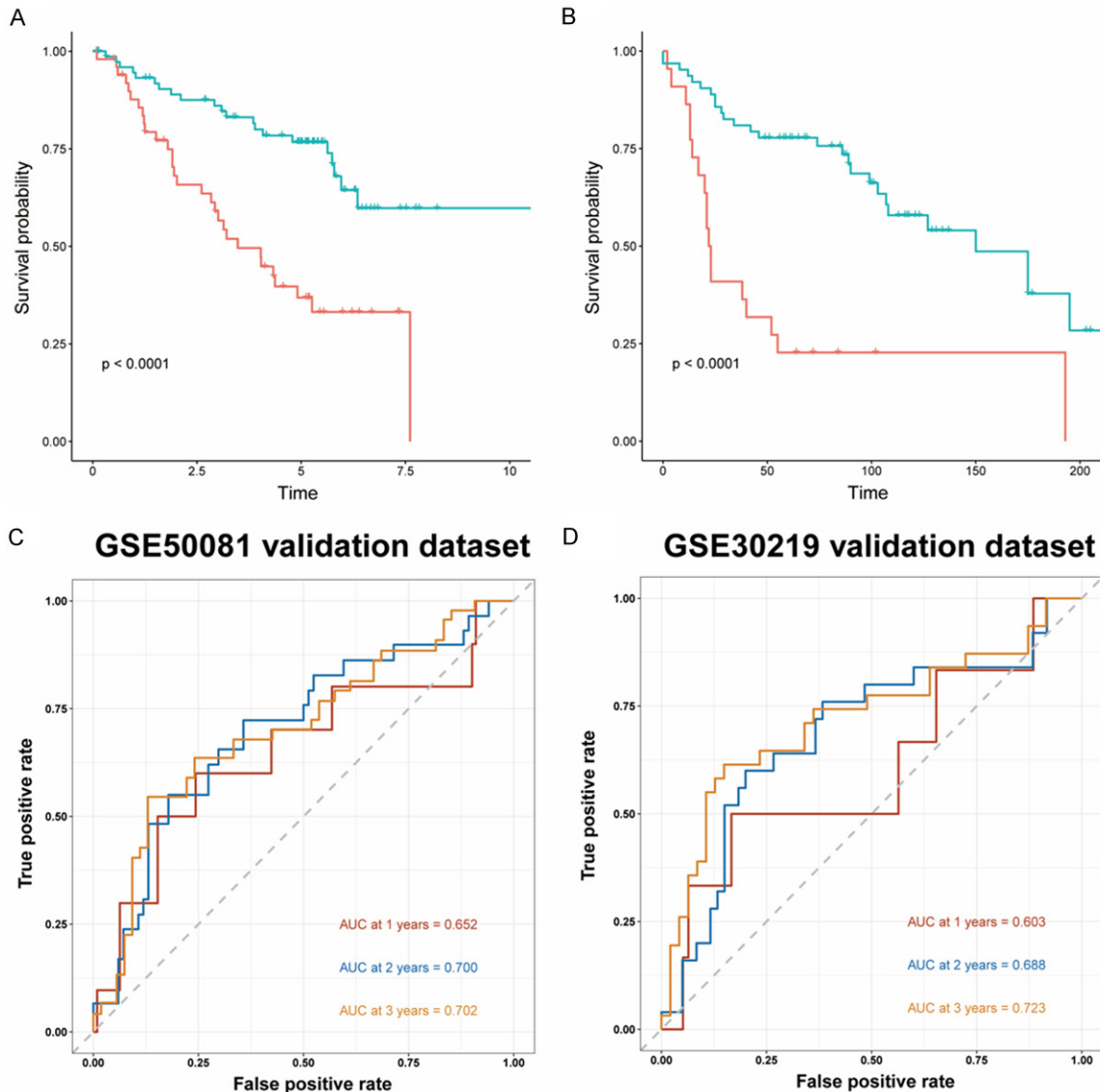


**Figure 4.** The prognostic performance of m6A-related signature was validated by the GSE50081 (A and B) and GSE30219 dataset (C and D).

(Figure 4A, 4B). The predictive power of the developed risk signature was also assessed by these two datasets. The ROC curves of GSE50081 dataset showed an AUC value of 0.70, 0.73 and 0.72 at 1-, 3-, and 5-year OS, respectively (Figure 4C). Similarly, GSE30219 dataset had an excellent prediction for 1-, 3-, and 5-year OS, with an AUC value of 0.75, 0.71 and 0.75, respectively (Figure 4D).

#### Enrichment analysis of m6A-related gene signature

Next, we set out to understand the signaling pathways characterized for risk signature of m6A-related genes. First, the GSEA analysis

was conducted to investigate the enriched signaling pathways. As shown in Figure 5A, the results revealed that several important molecular pathways, such as ESTROGEN\_RESPONSE\_LATE, REACTIVE\_OXYGEN\_SPECIES\_PATHWAY, JAK\_STAT3\_signaling, P53\_pathway and PI3K\_AKT\_mTOR\_signaling, which were greatly enriched in high-risk group (Figure 5A). Using the differentially expressed gene list of low vs. high-risk group, the Gene Ontology enrichment analysis was accomplished. The results further confirmed that genes that were differentially expressed were principally included in cytokinetic process, positive regulation of ATPase activity and icosanoid biosynthetic process (Figure 5B).



**A**

T cells CD4 memory activated

Macrophages M1

Macrophages M0

T cells CD8

Eosinophils

Mast cells activated

Dendritic cells activated

Macrophages M2

T cells CD4 memory resting

Monocytes

Dendritic cells resting

Mast cells resting

correlation

pvalue

abs(correlation)

**B**

HExp LExp

TP53

TTN

MUC16

RYR2

CDMD3

LRP1B

ZFYH4

USH2A

KIF3

SPD1A

ARX2

FLG

NAV3

COL11A1

ZNF336

FAT3

KEAP1

MUC7

PCDH15

CDMB1

ANKK2

APOL8

ADAMTS12

TNFR

RPL11

DNMB8

RAP82

PCLO

NRXN1

ADGRG4

Group

Alterations

Nonsense\_Mutation

Missense\_Mutation

Frame\_Shift\_Del

Frame\_Shift\_Ins

Splice\_Site

In\_Frame\_Del

Multi\_Hit

**C**

Estimated IC<sub>50</sub> of Bicalutamide

Wilcoxon,  $p = 2.4e-05$

LExp HExp

Expression of riskscore

Estimated IC<sub>50</sub> of Erlotinib

Wilcoxon,  $p = 1.4e-05$

LExp HExp

Expression of riskscore

Estimated IC<sub>50</sub> of Dasatinib

Wilcoxon,  $p = 0.48$

LExp HExp

Expression of riskscore

Estimated IC<sub>50</sub> of Lapatinib

Wilcoxon,  $p = 0.045$

LExp HExp

Expression of riskscore

Estimated IC<sub>50</sub> of AKT inhibitor VIII

Wilcoxon,  $p = 2.7e-05$

LExp HExp

Expression of riskscore

Estimated IC<sub>50</sub> of Imatinib

Wilcoxon,  $p = 4.7e-05$

LExp HExp

Expression of riskscore

**D**

ESR1

CDKN2A

CDKN2B

CDKN2C

CDKN2D

CDKN2E

CDKN2F

CDKN2G

CDKN2H

CDKN2I

CDKN2J

CDKN2K

CDKN2L

CDKN2M

CDKN2N

CDKN2O

CDKN2P

CDKN2Q

CDKN2R

CDKN2S

CDKN2T

CDKN2U

CDKN2V

CDKN2W

CDKN2X

CDKN2Y

CDKN2Z

CDKN2AA

CDKN2AB

CDKN2AC

CDKN2AD

CDKN2AE

CDKN2AF

CDKN2AG

CDKN2AH

CDKN2AI

CDKN2AJ

CDKN2AK

CDKN2AL

CDKN2AM

CDKN2AN

CDKN2AO

CDKN2AP

CDKN2AQ

CDKN2AR

CDKN2AS

CDKN2AT

CDKN2AU

CDKN2AV

CDKN2AW

CDKN2AX

CDKN2AY

CDKN2AZ

CDKN2BA

CDKN2BB

CDKN2BC

CDKN2BD

CDKN2BE

CDKN2BF

CDKN2BG

CDKN2BH

CDKN2BI

CDKN2BJ

CDKN2BK

CDKN2BL

CDKN2BM

CDKN2BN

CDKN2BO

CDKN2BP

CDKN2BQ

CDKN2BR

CDKN2BS

CDKN2BT

CDKN2BU

CDKN2BV

CDKN2BW

CDKN2BX

CDKN2BY

CDKN2BZ

CDKN2CA

CDKN2CB

CDKN2CC

CDKN2CD

CDKN2CE

CDKN2CF

CDKN2CG

CDKN2CH

CDKN2CI

CDKN2CJ

CDKN2CK

CDKN2CL

CDKN2CM

CDKN2CN

CDKN2CO

CDKN2CP

CDKN2CQ

CDKN2CR

CDKN2CS

CDKN2CT

CDKN2CU

CDKN2CV

CDKN2CW

CDKN2CX

CDKN2CY

CDKN2CZ

CDKN2DA

CDKN2DB

CDKN2DC

CDKN2DD

CDKN2DE

CDKN2DF

CDKN2DG

CDKN2DH

CDKN2DI

CDKN2DJ

CDKN2DK

CDKN2DL

CDKN2DM

CDKN2DN

CDKN2DO

CDKN2DP

CDKN2DQ

CDKN2DR

CDKN2DS

CDKN2DT

CDKN2DU

CDKN2DV

CDKN2DW

CDKN2DX

CDKN2DY

CDKN2DZ

CDKN2EA

CDKN2EB

CDKN2EC

CDKN2ED

CDKN2EE

CDKN2EF

CDKN2EG

CDKN2EH

CDKN2EI

CDKN2EJ

CDKN2EK

CDKN2EL

CDKN2EM

CDKN2EN

CDKN2EO

CDKN2EP

CDKN2EQ

CDKN2ER

CDKN2ES

CDKN2ET

CDKN2EU

CDKN2EV

CDKN2EW

CDKN2EX

CDKN2EY

CDKN2EZ

CDKN2FA

CDKN2FB

CDKN2FC

CDKN2FD

CDKN2FE

CDKN2FF

CDKN2FG

CDKN2FH

CDKN2FI

CDKN2FJ

CDKN2FK

CDKN2FL

CDKN2FM

CDKN2FN

CDKN2FO

CDKN2FP

CDKN2FQ

CDKN2FR

CDKN2FS

CDKN2FT

CDKN2FU

CDKN2FV

CDKN2FW

CDKN2FX

CDKN2FY

CDKN2FZ

CDKN2GA

CDKN2GB

CDKN2GC

CDKN2GD

CDKN2GE

CDKN2GF

CDKN2GG

CDKN2GH

CDKN2GI

CDKN2GJ

CDKN2GK

CDKN2GL

CDKN2GM

CDKN2GN

CDKN2GO

CDKN2GP

CDKN2GQ

CDKN2GR

CDKN2GS

CDKN2GT

CDKN2GU

CDKN2GV

CDKN2GW

CDKN2GX

CDKN2GY

CDKN2GZ

CDKN2HA

CDKN2HB

CDKN2HC

CDKN2HD

CDKN2HE

CDKN2HF

CDKN2HG

CDKN2HH

CDKN2HI

CDKN2HJ

CDKN2HK

CDKN2HL

CDKN2HM

CDKN2HN

CDKN2HO

CDKN2HP

CDKN2HQ

CDKN2HR

CDKN2HS

CDKN2HT

CDKN2HU

CDKN2HV

CDKN2HW

CDKN2HX

CDKN2HY

CDKN2HZ

CDKN2IA

CDKN2IB

CDKN2IC

CDKN2ID

CDKN2IE

CDKN2IF

CDKN2IG

CDKN2IH

CDKN2II

CDKN2IJ

CDKN2IK

CDKN2IL

CDKN2IM

CDKN2IN

CDKN2IO

CDKN2IP

CDKN2IQ

CDKN2IR

CDKN2IS

CDKN2IT

CDKN2IU

CDKN2IV

CDKN2IW

CDKN2IX

CDKN2IY

CDKN2IZ

CDKN2JA

CDKN2JB

CDKN2JC

CDKN2JD

CDKN2JE

CDKN2JF

CDKN2JG

CDKN2JH

CDKN2JI

CDKN2JJ

CDKN2JK

CDKN2JL

CDKN2JM

CDKN2JN

CDKN2JO

CDKN2JP

CDKN2JQ

CDKN2JR

CDKN2JS

CDKN2JT

CDKN2JU

CDKN2JV

CDKN2JW

CDKN2JX

CDKN2JY

CDKN2JZ

CDKN2KA

CDKN2KB

CDKN2KC

CDKN2KD

CDKN2KE

CDKN2KF

CDKN2KG

CDKN2KH

CDKN2KI

CDKN2KJ

CDKN2KK

CDKN2KL

CDKN2KM

CDKN2KN

CDKN2KO

CDKN2KP

CDKN2KQ

CDKN2KR

CDKN2KS

CDKN2KT</

### Immune cell infiltration, chemosensitivity and genetic features of groups under different risk categories

infiltration mediation during tumor development. This further provoked us to understand the relationship between m6A-linked genetic hallmarks and immune cell infiltration to explore whether this pathway is involved in LUAD. Our results demonstrated that high-risk patients

had larger proportion of activated immune cells like memory T cells activated by CD4+, macrophages like M1 and M0, CD8+ T cells, eosinophils and activated mast cells. In contrast, activated and resting dendritic cells, M2 macrophages, monocytes and naïve mast cells at resting stage were decreased to a great extent in patients from high-risk category (**Figure 5C**). Single nucleotide variations (SNVs) were further analyzed in high- and low-risk groups, and it was revealed that individuals from the said group displayed a frequent mutation of TP53 (52%) and TTN (47%) (**Figure 5D**). Furthermore, **Figure 5E** shows the relation of chemotherapeutic drug sensitivity with the risk score of individuals. Patients from high-risk category had a high drug-resistance to Bicalutamide, Erlotinib, Dasatinib, Lapatinib, AKT inhibitor VIII and Imatinib than the low-risk patients (**Figure 5E**).

#### *Gene expression of HNRNPC, IGF2BP1 and IGF2BP2 in pan-cancer samples*

We assessed the expression and predictive value of the three m6A genes in pan-cancer samples. The expression levels of HNRNPC, IGF2BP1 and IGF2BP2 in 33 types of pan-cancer samples were detected using the GEPIA online tool. The results verified that the extent of expression of the corresponding genes were greatly elevated in most of tumor tissues, including both lung squamous cell carcinoma (LUSC) and LUAD (**Figure 6**).

#### *Effects of HNRNPC expression on biological behaviors of LUAD cells*

Although previous evidence has shown that several m6A-related genes were associated with the development and progression of human cancers, there was no study to explore the biological roles of HNRNPC in LUAD. The present findings revealed a higher expression level of HNRNPC in three LUAD cell lines in comparison to that in normal lung epithelial cell lines ( $P<0.001$ ) (**Figure 7A**). Furthermore, the formation of colony assay represented that the growth of A549 cells was considerably enhanced by HNRNPC overexpression and was reduced by silencing of HNRNPC expression ( $P<0.001$ ) (**Figure 7B**). Moreover, the results indicated that overexpression of HNRNPC also considerably promoted the migration as well as the cellular invasion, while the loss of HNRNPC

expression inhibited these malignant phenotypes in LUAD cells ( $P<0.001$ ) (**Figure 7C, 7D**).

#### **Discussion**

Lung cancer is a major health challenge for both males and females around the world [1, 2]. It is urgent to develop novel and more accurate molecular markers for early diagnostic intervention and prognostic assessment. Recently, increasing evidence has suggested that m6A modifications have an impact on biological behaviors of lung cancer cells by regulating gene expression [19-21], suggesting that exploration of molecular features and prognostic importance of genes related to m6A can be helpful for understanding the role of the said pathway in the progression of human cancers.

We found herein that nearly all the studied m6A-related genes were differentially expressed and had a high mutation frequency in LUAD samples, suggesting that these regulators of the m6A alterations are important factors in the pathogenesis of this malignancy. According to the m6A-related gene expressions, we assigned patients with LUAD in two subgroups, and survival analysis revealed a significant prognostic difference between the two groups. These data suggested that there was a strong correlation between LUAD prognosis and pathway associated with modification of m6A-related genes. Therefore, we further evaluated their prognostic significance and developed a prognostic gene expression signature based on three m6A regulators (IGF2BP1, IGF2BP2 and HNRNPC). The prognostic signature demonstrated a suitable predictive power for the prognosis of patients with LUAD, and there was significant correlation between high-risk score and poor OS. More importantly, the prognostic value of m6A-related signature was corroborated by other two independent cohorts. These outcomes confirmed that the m6A diagnostic hallmarks could be used as a promising marker for therapeutic assessment in patients with LUAD.

As m6A “readers”, IGF2BP1, IGF2BP2 and HNRNPC were identified as RNA-binding proteins for recognizing and binding to m6A sites. It has been reported that IGF2BP1 and IGF2BP2 are mainly associated with RNA stability, and they function as oncogenes in lung cancer [22-25]. Recently, Zhang et al. reported that

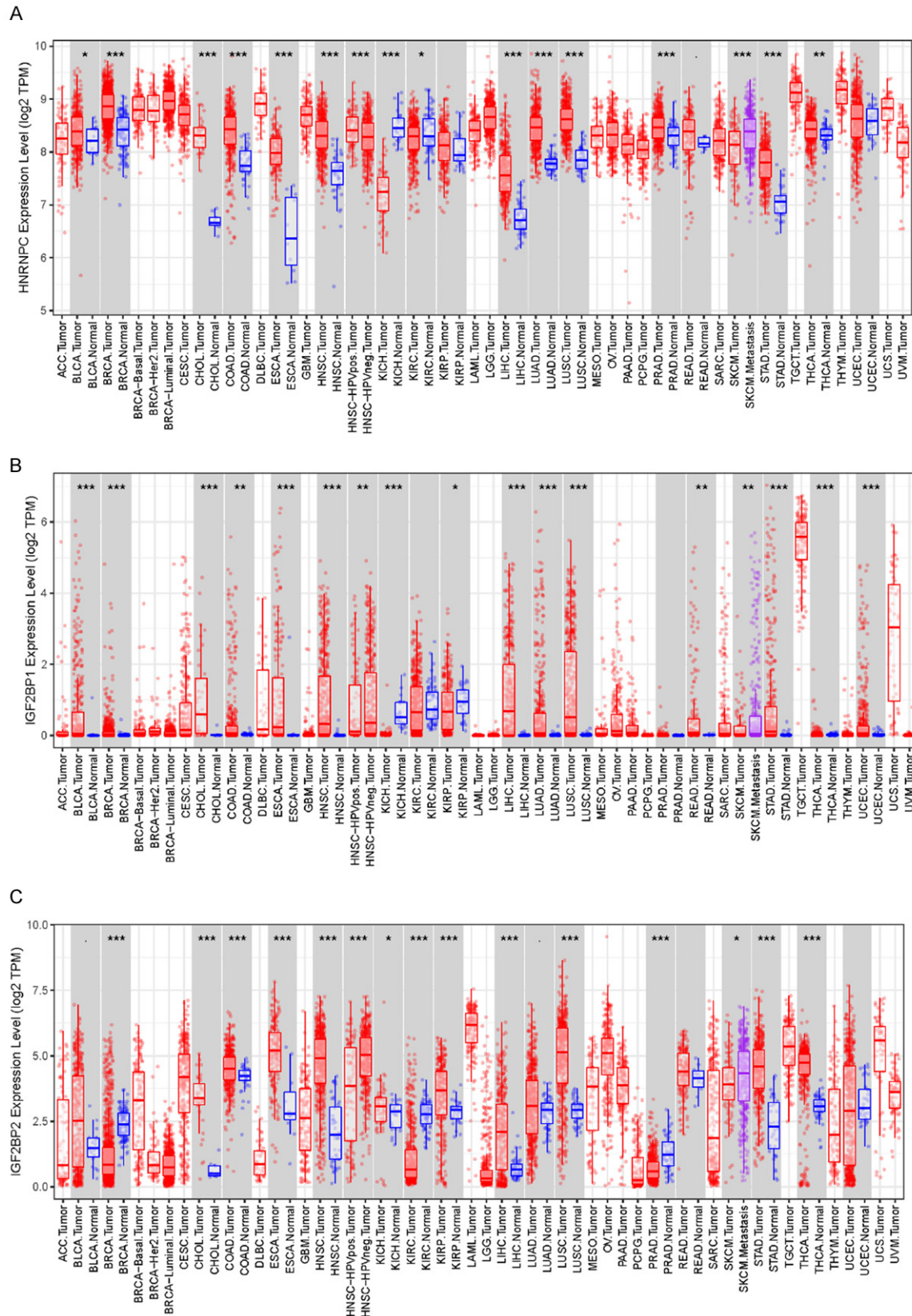


**Figure 6.** The expression of HNRNPC (A), IGF2BP1 (B) and IGF2BP2 (C) in the pan-cancer samples. \* $P < 0.05$ , \*\* $P < 0.01$ , and \*\*\* $P < 0.001$ .



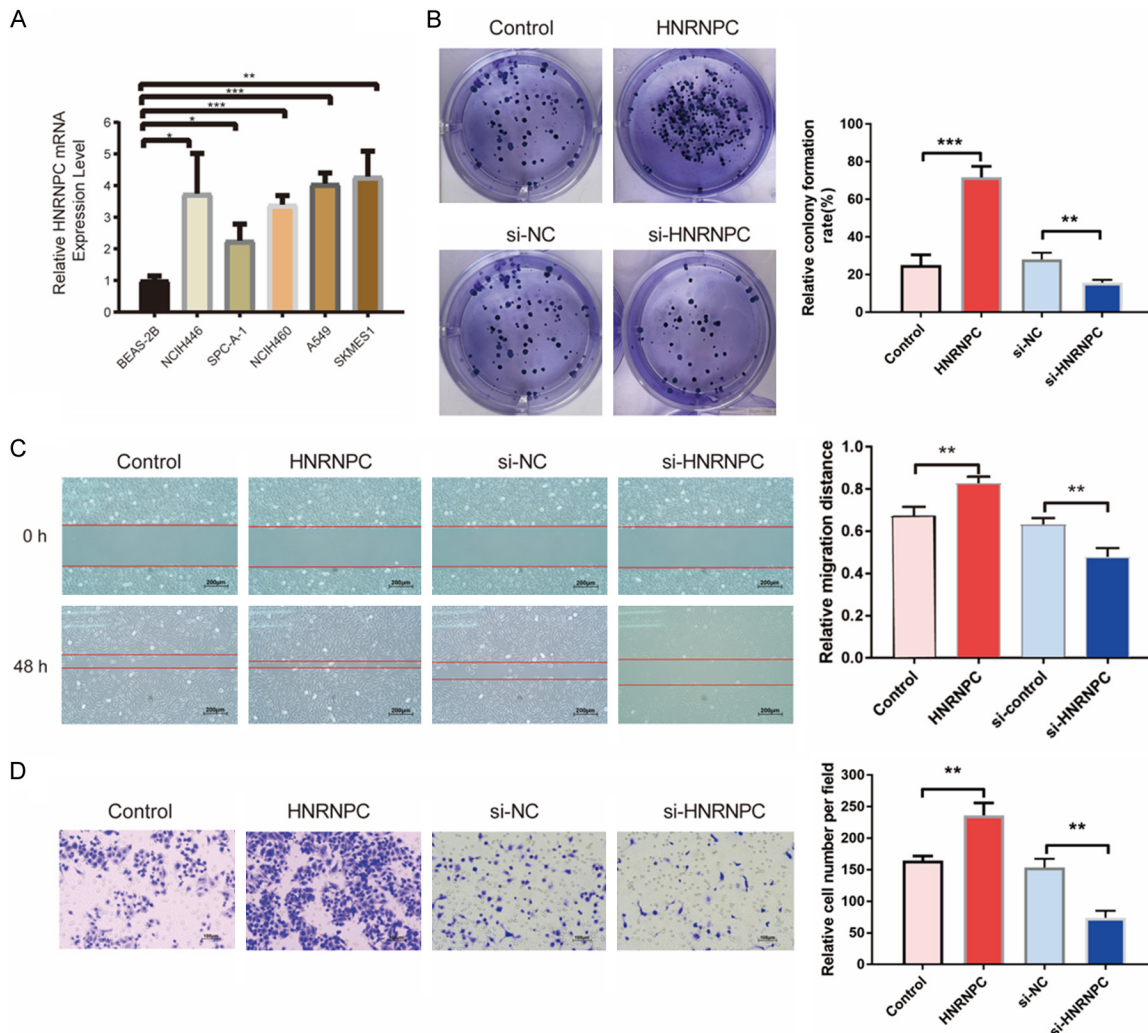


**Figure 7.** The expression levels of HNRNPC in LUAD cell lines (A) and its influences on cell growth (B), migration (C) and invasion (D) of A549 cells in vitro. \* $P < 0.05$ , \*\* $P < 0.01$ , and \*\*\* $P < 0.001$ .

IGF2BP1 silencing leads to significant reduction in cell proliferation, migration and also cellular invasion, which can further induce cell cycle arrest and ultimately cause the cellular death of non-small cell lung cancer (NSCLC) cells [22]. Huang et al. reported that IGF2BP2 served as a direct target of miR-485-5p to promote the growth and metastasis of NSCLC [24]. In our study, the results further confirmed that the levels of IGF2BP1 and 2 increased markedly in LUAD samples, and there was an obvious relationship between the high expression and poor survival. These findings consistently suggested that IGF2BP1 and IGF2BP2 could significantly affect the development of lung cancer.

As per previous analysis, the heterogenous nuclear ribonucleoprotein C, also known as

(HNRNPC), was involved in regulation of pre-mRNA processing, translation and splicing [26, 27]. It has been shown that the expression of HNRNPC was dysregulated in ovarian cancer, oral squamous cell carcinoma and glioblastoma multiforme [28-30]. However, its prognostic significance and biological roles in LUAD remain unclear. In the present research, it is observed that HNRNPC transcription was considerably increased in LUAD tissue than that in normal samples, and the increased expression of HNRNPC was associated with worse OS in patients with LUAD. These results confirmed that HNRNPC could exhibit as an oncogenic factor in the occurrence and progression of LUAD. To further validate this hypothesis, we investigated its biological roles in lung cancer cells. Consistent with the findings of bioinformatic analysis, the expression of HNRNPC was

also significantly raised in cellular models of lung cancer compared to that in normal lung epithelial cells. More importantly, the silencing of HNRNPC expression exerts an inhibitory effect on cell proliferation and migration of LUAD in vitro. The outcomes promoted a need to further explore the potential targets of HNRNPC in the upstream and downstream and its biological roles in vivo.

To dissect the molecular mechanisms of the three m6A modifiers, we conducted the GSVA analysis. Unsurprisingly, these m6A-related genes were greatly enriched in several well-known cancer-related signaling, including JAK/STAT3 pathway, P53 pathway and PI3K/AKT/mTOR pathway. These observations might provide us a potential insight for biological roles of these m6A regulators in LUAD. In addition to surgical resection, the current treatment options for patients with lung cancer included chemotherapy, targeted therapy and immunotherapy. It is of great importance to identify patients who might potentially need adjuvant treatment. The present study assessed the relationships between patients with different risk score and their reported sensitivity to chemotherapy drugs, and the results confirmed that the high-risk patients were more resistant to Bicalutamide, Erlotinib, Dasatinib, Lapatinib, AKT inhibitor VIII and Imatinib. These results might provide useful guidance for the individualized treatment of LUAD. Moreover, the present findings showed that high-risk score was considerably related to the enhanced immune cell infiltration (e.g., M1 macrophages, CD8+ T cells and M0 macrophage) and TP53 mutation. Previous evidence has shown that immune cell infiltration was involved in the carcinogenesis and tumor progression, and blockade of immune checkpoints such as anti PD-1 and anti CTLA-4 are becoming a promising treatment strategy for lung cancer [31, 32]. Our results suggested that m6A regulators can affect remarkably the tumor immune microenvironment, and the risk signature might help us determine the response to immunotherapy.

In conclusion, the current study assessed the transcription, prognostic value and multiomic properties of m6A regulators in patients with LUAD from the public TCGA dataset. We identified and confirmed a prognostic signature according to 3 m6A regulators (IGF2BP1, IGF2BP2 and HNRNPC), and it was found that

the risk signature could be utilized for more accurate OS prediction. Moreover, we represented the efficient performance of m6A-related signature in chemotherapeutic resistance, tumor microenvironment and genetic mutation. Our findings give deep insight into the prognostic value of gene expression and individualized treatment options for patients with LUAD.

## Acknowledgements

This study was supported by National Natural Science Foundation of China (81860534); Natural Science Foundation of Inner Mongolia (2021MS08152); Inner Mongolia Autonomous Region science and technology planning project (2019GG039, 2019GG086, 2021GG0167); Program for Young Talents of Science and Technology in Universities of Inner Mongolia Autonomous Region (NJYT22004); Health science and technology planning project of Inner Mongolia Autonomous Region (2022-01356); Zhi Yuan Talent Projects of Inner Mongolia Medical University (ZY0202011); Science and Technology achievement transformation Project of Inner Mongolia Medical University (YKD2019CGZH004).

## Disclosure of conflict of interest

None.

**Address correspondence to:** Hao Yang, Department of Radiation Oncology, Inner Mongolia Cancer Hospital & Affiliated People's Hospital of Inner Mongolia Medical University, Huhhot 010020, Inner Mongolia Autonomous Region, China. E-mail: haoyang050201@163.com; Hongwei Cui, Scientific Research Department, Inner Mongolia Cancer Hospital & Affiliated People's Hospital of Inner Mongolia Medical University, Huhhot 010020, Inner Mongolia Autonomous Region, China. E-mail: cuihw2001423@163.com

## References

- [1] Siegel RL, Miller KD, Fuchs HE and Jemal A. Cancer statistics, 2021. *CA Cancer J Clin* 2021; 71: 7-33.
- [2] Sung H, Ferlay J, Siegel RL, Laversanne M, Soerjomataram I, Jemal A and Bray F. Global cancer statistics 2020: GLOBOCAN estimates of incidence and mortality worldwide for 36 cancers in 185 countries. *CA Cancer J Clin* 2021; 71: 209-249.
- [3] Chen W, Zheng R, Baade PD, Zhang S, Zeng H, Bray F, Jemal A, Yu XQ and He J. Cancer statis-



- tics in China, 2015. *CA Cancer J Clin* 2016; 66: 115-132.
- [4] Goldstraw P, Chansky K, Crowley J, Rami-Porta R, Asamura H, Eberhardt WE, Nicholson AG, Groome P, Mitchell A and Bolejack V; International Association for the Study of Lung Cancer Staging and Prognostic Factors Committee, Advisory Boards, and Participating Institutions; International Association for the Study of Lung Cancer Staging and Prognostic Factors Committee Advisory Boards and Participating Institutions. The IASLC lung cancer staging project: proposals for revision of the TNM stage groupings in the forthcoming (eighth) edition of the TNM classification for lung cancer. *J Thorac Oncol* 2016; 11: 39-51.
- [5] Wang X, Lu Z, Gomez A, Hon GC, Yue Y, Han D, Fu Y, Parisien M, Dai Q, Jia G, Ren B, Pan T and He C. N6-methyladenosine-dependent regulation of messenger RNA stability. *Nature* 2014; 505: 117-120.
- [6] Adhikari S, Xiao W, Zhao YL and Yang YG. M(6)A: signaling for mRNA splicing. *RNA Biol* 2016; 13: 756-759.
- [7] Roundtree IA, Evans ME, Pan T and He C. Dynamic RNA modifications in gene expression regulation. *Cell* 2017; 169: 1187-1200.
- [8] Yang Y, Hsu PJ, Chen YS and Yang YG. Dynamic transcriptomic m6A decoration: writers, erasers, readers and functions in RNA metabolism. *Cell Res* 2018; 28: 616-624.
- [9] Batista PJ. The RNA modification N6-methyladenosine and its implications in human disease. *Genomics Proteomics Bioinformatics* 2017; 15: 154-163.
- [10] Chen XY, Zhang J and Zhu JS. The role of m6A RNA methylation in human cancer. *Mol Cancer* 2019; 18: 103.
- [11] Xie F, Huang C, Liu F, Zhang H, Xiao X, Sun J, Zhang X and Jiang G. CircPTPRA blocks the recognition of RNA N6-methyladenosine through interacting with IGF2BP1 to suppress bladder cancer progression. *Mol Cancer* 2021; 20: 68.
- [12] Yu H, Yang X, Tang J, Si S, Zhou Z, Lu J, Han J, Yuan B, Wu Q, Lu Q and Yang H. ALKBH5 inhibited cell proliferation and sensitized bladder cancer cells to cisplatin by m6A-CK2 $\alpha$ -mediated glycolysis. *Mol Ther Nucleic Acids* 2020; 23: 27-41.
- [13] Jin Y, Wang Z, He D, Zhu Y, Hu X, Gong L, Xiao M, Chen X, Cheng Y and Cao K. Analysis of m6A-related signatures in the tumor immune microenvironment and identification of clinical prognostic regulators in adrenocortical carcinoma. *Front Immunol* 2021; 12: 637933.
- [14] Der SD, Sykes J, Pintilie M, Zhu CQ, Strumpf D, Liu N, Jurisica I, Shepherd FA and Tsao MS. Validation of a histology-independent prognostic gene signature for early-stage, non-small-cell lung cancer including stage IA patients. *J Thorac Oncol* 2014; 9: 59-64.
- [15] Rousseaux S, Debernardi A, Jacquiau B, Vitte AL, Vesin A, Nagy-Mignotte H, Moro-Sibilot D, Bricchon PY, Lantuejoul S, Hainaut P, Laffaire J, de Reyniès A, Beer DG, Timsit JF, Brambilla C, Brambilla E and Khochbin S. Ectopic activation of germline and placental genes identifies aggressive metastasis-prone lung cancers. *Sci Transl Med* 2013; 5: 186ra66.
- [16] Gao J, Aksoy BA, Dogrusoz U, Dresdner G, Gross B, Sumer SO, Sun Y, Jacobsen A, Sinha R, Larsson E, Cerami E, Sander C and Schultz N. Integrative analysis of complex cancer genomics and clinical profiles using the cBioPortal. *Sci Signal* 2013; 6: p11.
- [17] Becht E, Giraldo NA, Lacroix L, Buttard B, Elarouci N, Petitprez F, Selves J, Laurent-Puig P, Sautès-Fridman C, Fridman WH and de Reyniès A. Estimating the population abundance of tissue-infiltrating immune and stromal cell populations using gene expression. *Genome Biol* 2016; 17: 218.
- [18] Yang W, Soares J, Greninger P, Edelman EJ, Lightfoot H, Forbes S, Bindal N, Beare D, Smith JA, Thompson IR, Ramaswamy S, Futreal PA, Haber DA, Stratton MR, Benes C, McDermott U and Garnett MJ. Genomics of drug sensitivity in cancer (GDSC): a resource for therapeutic biomarker discovery in cancer cells. *Nucleic Acids Res* 2013; 41: D955-961.
- [19] Li Y, Sheng H, Ma F, Wu Q, Huang J, Chen Q, Sheng L, Zhu X, Zhu X and Xu M. RNA m(6)A reader YTHDF2 facilitates lung adenocarcinoma cell proliferation and metastasis by targeting the AXIN1/Wnt/ $\beta$ -catenin signaling. *Cell Death Dis* 2021; 12: 479.
- [20] Ma L, Chen T, Zhang X, Miao Y, Tian X, Yu K, Xu X, Niu Y, Guo S, Zhang C, Qiu S, Qiao Y, Fang W, Du L, Yu Y and Wang J. The m6A reader YTHDC2 inhibits lung adenocarcinoma tumorigenesis by suppressing SLC7A11-dependent antioxidant function. *Redox Biol* 2021; 38: 101801.
- [21] Li H, Zhang Y, Guo Y, Liu R, Yu Q, Gong L, Liu Z, Xie W and Wang C. ALKBH1 promotes lung cancer by regulating m6A RNA demethylation. *Biochem Pharmacol* 2021; 189: 114284.
- [22] Zhang J, Luo W, Chi X, Zhang L, Ren Q, Wang H and Zhang W. IGF2BP1 silencing inhibits proliferation and induces apoptosis of high glucose-induced non-small cell lung cancer cells by regulating Netrin-1. *Arch Biochem Biophys* 2020; 693: 108581.
- [23] Huang Q, Guo H, Wang S, Ma Y, Chen H, Li H, Li J, Li X, Yang F, Qiu M, Zhao S and Wang J. A novel circular RNA, circXPO1, promotes lung adenocarcinoma progression by interacting with IGF2BP1. *Cell Death Dis* 2020; 11: 1031.

- [24] Huang RS, Zheng YL, Li C, Ding C, Xu C and Zhao J. MicroRNA-485-5p suppresses growth and metastasis in non-small cell lung cancer cells by targeting IGF2BP2. *Life Sci* 2018; 199: 104-111.
- [25] Ma YS, Shi BW, Guo JH, Liu JB, Yang XL, Xin R, Shi Y, Zhang DD, Lu GX, Jia CY, Wang HM, Wang PY, Yang HQ, Zhang JJ, Wu W, Cao PS, Yin YZ, Gu LP, Tian LL, Lv ZW, Wu CY, Wang GR, Yu F, Hou LK, Jiang GX and Fu D. MicroRNA-320b suppresses HNF4G and IGF2BP2 expression to inhibit angiogenesis and tumor growth of lung cancer. *Carcinogenesis* 2021; 42: 762-771.
- [26] Fischl H, Neve J, Wang Z, Patel R, Louey A, Tian B and Furger A. HnRNP regulates cancer-specific alternative cleavage and polyadenylation profiles. *Nucleic Acids Res* 2019; 47: 7580-7591.
- [27] Cieniková Z, Jayne S, Damberger FF, Allain FH and Maris C. Evidence for cooperative tandem binding of hnRNP C RRM in mRNA processing. *RNA* 2015; 21: 1931-1942.
- [28] Kleemann M, Schneider H, Unger K, Sander P, Schneider EM, Fischer-Posovszky P, Handrick R and Otte K. MiR-744-5p inducing cell death by directly targeting HNRNPC and NFIX in ovarian cancer cells. *Sci Rep* 2018; 8: 9020.
- [29] Huang GZ, Wu QQ, Zheng ZN, Shao TR, Chen YC, Zeng WS and Lv XZ. M6A-related bioinformatics analysis reveals that HNRNPC facilitates progression of OSCC via EMT. *Aging (Albany NY)* 2020; 12: 11667-11684.
- [30] Wang LC, Chen SH, Shen XL, Li DC, Liu HY, Ji YL, Li M, Yu K, Yang H, Chen JJ, Qin CZ, Luo MM, Lin QX and Lv QL. M6A RNA methylation regulator HNRNPC contributes to tumorigenesis and predicts prognosis in glioblastoma multiforme. *Front Oncol* 2020; 10: 536875.
- [31] Lei X, Lei Y, Li JK, Du WX, Li RG, Yang J, Li J, Li F and Tan HB. Immune cells within the tumor microenvironment: biological functions and roles in cancer immunotherapy. *Cancer Lett* 2020; 470: 126-133.
- [32] Gun SY, Lee SWL, Sieow JL and Wong SC. Targeting immune cells for cancer therapy. *Redox Biol* 2019; 25: 101174.